Microstructure Characterization of Aged Heat Resistant Steels

Maribel L. Saucedo-Muñoz, Arturo Ortiz-Mariscal, Victor M. Lopez-Hirata, Jose D. Villegas-Cardenas and Ana Maria Paniagua-Mercado

Abstract The precipitation evolution was studied experimentally and numerically during aging of as-cast heat resistant steel at 700, 800 and 900 °C. Thermo-Calc result showed a good assessment of the non-equilibrium phases for as-cast HK40 steels in comparison to the experimental results. In contrast, the Time-Temperature-Precipitation diagram for the $M_{23}C_6$ precipitation calculated with PRISMA showed a good agreement with the experimental growth kinetics precipitation for the steel after aging at 700, 800 and 900 °C.

Keywords Carbide precipitation · Isothermal aging · As-cast Heat resistant steels

Introduction

Heat-resistant type steels are used usually in the as-cast condition and they were developed to be used at high temperatures of 700–900 °C for prolonged times. This exposure may cause the deterioration of microstructure [1]. For instance, HK40 and HP40 steels are examples of heat resistant steels which have been applied to fabricate different industrial components [2]. These components may failure because of creep damage, metal dusting creep fatigue and the presence of brittle phases, among other causes [3–5]. The microstructure changes usually occurs during heating of these steels [4]. Several works [6, 7] have been conducted to study the microstructure evolution in this steel. Thermo-Calc softwares [8] have been utilized successfully to analyze not only the phase stability in the equilibrium and non-equilibrium (as-cast) conditions, but also the precipitation kinetics in different alloys at the service temperatures. PRISMA software permits to calculate

M. L. Saucedo-Muñoz · A. Ortiz-Mariscal · V. M. Lopez-Hirata (✉)
J. D. Villegas-Cardenas · A. M. Paniagua-Mercado
Instituto Politécnico Nacional (ESIQIE-ESFM), UPALM Edif. 7,
Mexico City 07300, Mexico
e-mail: vlopezhi@prodigy.net.mx

The Minerals, Metals & Materials Society, *TMS 2018 147th Annual Meeting & Exhibition Supplemental Proceedings*, The Minerals, Metals & Materials Series,
https://doi.org/10.1007/978-3-319-72526-0_76

numerically the growth kinetics of precipitation and the precipitation results can be summarized in Time-Temperature-Precipitation TTP diagram. Thus, the purpose of the present work is to analyze microstructural and numerically the formed phase in two heat-resistant steels, HK40 and the precipitation evolution during the isothermal aging at 700, 800 and 900 °C for different times.

Experimental Procedure

The chemical composition of the HK40 steel is shown in Table 1. Specimens of approximately 10 × 10 × 10 mm were cut from the cast ingot. These specimens were aged at 700, 800 and 900 °C for times up to 2000 h in an electric tubular furnace. The as-cast and aged specimens were prepared metallographically, etched with Kalling etchant, and then observed with both light (LM) and scanning electron (SEM) microscopes. Energy-Dispersive X-ray (EDX) analysis was used to determine the chemical composition of some precipitates in the steel specimens. Some specimens were also analyzed by X-Ray Diffraction (DRX) with Cr Kα radiation.

Precipitate size was determined using SEM micrographs with a commercial software installed in a PC. A Thermo-Cal and PRISMA analyses were conducted for the phase formation and precipitation of HK40 [9].

Results and Discussion

Microstructural Characterization of Precipitation

Figure 1 shows the SEM micrographs of the microstructure evolutions for HK40 steel aged at 700, 800 and 900 °C for times up to 1500 h. SEM micrograph of as-cast steel indicates the presence primary carbides in the interdendritic zones and dendrites of the austenite matrix This primary carbides show an interlamellar morphology because they are formed by a eutectic reaction, as will be explained later. XRD diffractogram is shown in Fig. 2 for as-cast steel and it indicates the presence of XRD peaks corresponding to the austenite matrix and M_7C_3 carbides.

The aging process causes the precipitation of secondary carbides in the austenite matrix. These carbides have a cuboid morphology at the beginning of aging and it changes to rectangular plates with aging time. These plates show a crystallographic alignment with the austenite matrix [10]. The size of precipitates increases with aging time and temperature, as shown in Fig. 3. The coarsening process of

Table 1 Chemical composition in wt% of steel

Steel	C	Mn	Si	Cr	Ni	Nb	Ti
HK40	0.40	1.50	1.60	25.00	20.00	–	–

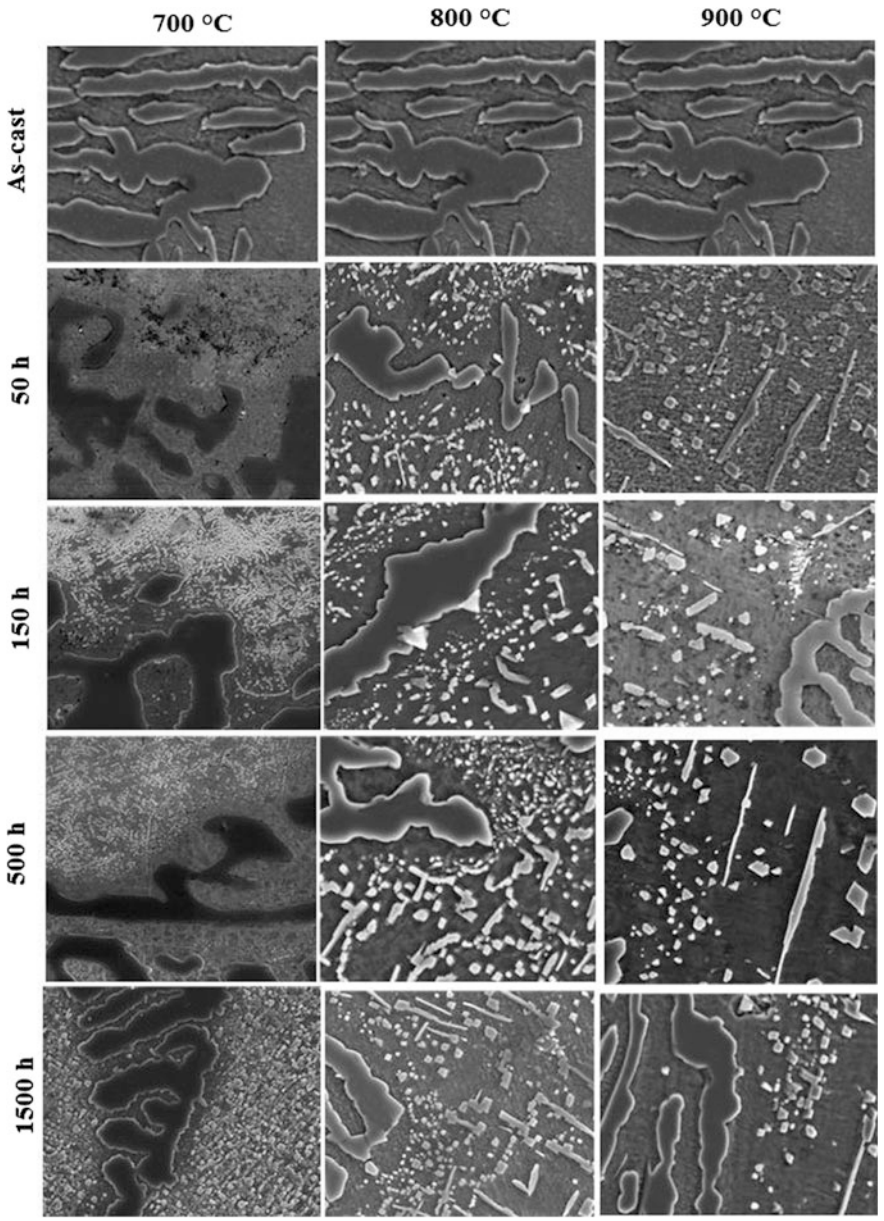

Fig. 1 SEM micrographs of the aged at 700, 800 and 900 °C for different times

secondary carbides is notorious during aging at 800 and 900 °C for long aging times. The decrease in the density of precipitates is clearly observed for these cases. Figure 5 shows the variation of radius to cube versus aging time having a linear

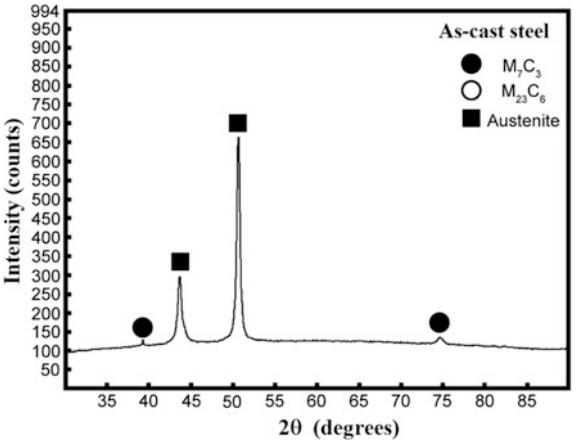

Fig. 2 XRD diffractogram of the as-cast steel

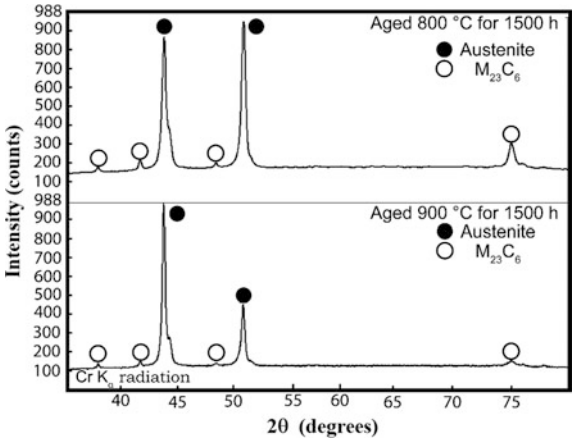

Fig. 3 XRD diffractograms of the steel aged at 800 and 900 °C

dependence which suggests that the coarsening of secondary carbides is a diffusion-controlled process as predicted by the Lifshitz-Slyozov-Wagner theory [11]. The primary carbides are observed to be gradually dissolved with aging time. XRD diffractograms for the specimens aged at 800 and 900 °C for 1500 h, as shown in Fig. 3, which indicates that the precipitates correspond to $M_{23}C_6$ carbides for both specimens.

The EDS-SEM element mapping images of the steel in the condition of as-cast and aged at 700 °C for different times is shown in Fig. 4. This figure shows clearly that the primary carbides are mainly composed of Cr; however, the presence of Mn is also noted. The chemical composition of secondary carbides is not clearly distinguished in Fig. 4. Nevertheless, SEM-EDS analysis reveals that are mainly composed of Cr and Fe.

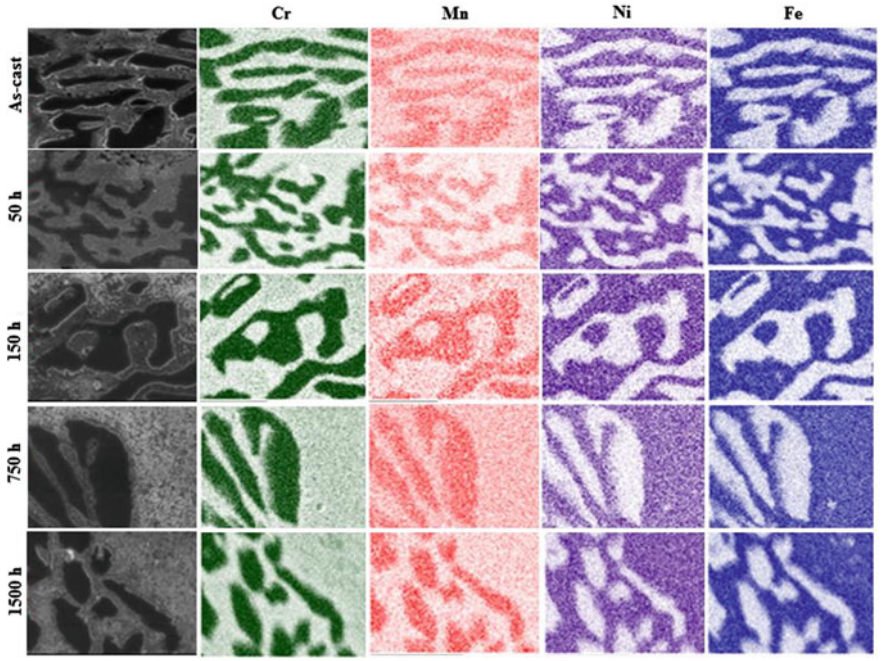

Fig. 4 EDS-elemental mapping for the as-cast steel and aged at 700 °C for different times

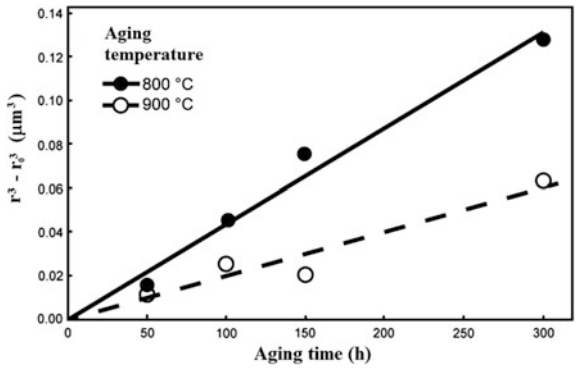

Fig. 5 Plot of r^3 versus aging time for the steel aged at 800 and 900 °C

The previous characterization results point out that the secondary $M_{23}C_6$ carbides are formed by the following precipitation reaction:

$$\gamma \rightarrow \gamma + M_{23}C_6 \tag{1}$$

That is the formation of $M_{23}C_6$ precipitates is useful to increase the creep strength of the steel when is in-service operation at high temperatures.

Thermo-Calc and PRISMA Analysis

The analysis of solidification for the steel was carried out based on the Scheil-Guiliver equation [8]. This analysis permits to determine the non-equilibrium phases formed during the alloy solidification. For instance, Fig. 6 shows the plot of temperature against the mole fraction of all phases. This figure indicates that the first solid phase is the austenite (FCC_A1#1 in Thermo-Calc designation) dendrites and subsequently the primary carbide M_7C_3 is formed following the eutectic reaction: $L \rightarrow \gamma + M_7C_3$. Furthermore, Themo-Calc predicts that the eutectic reaction takes place at approximately 1260 °C which is in good agreement with the literature [6]. The presence of this lamellar microconstituent is also observed in as-cast steel, Fig. 1. Thermo-Calc also shows that the carbides are not only formed by C, but also Mn content is also present which is in agreement with Fig. 4. As the temperature decreases, Fig. 6 shows that the M23C6 can precipitate from the supersaturated austenite matrix. The delta ferrite phase (BCC_A2) can also be present at low temperatures in a low volume fraction. This phase was not detected by XRD analysis of Fig. 2.

Figure 7 shows the equilibrium isoplethic or pseudobinary Fe-Cr phase diagram calculated by Thermo-Calc. This diagram shows clearly that the γ austenite and $M_{23}C_6$ carbides (FCC_A1#1 and M23C6) are the equilibrium phases expected for the steel composition at temperatures between 700 and 900 °C. These phases are consistent with the phases detected in the steel aged at 800 and 900 °C for 1500 h. This also confirms the precipitation reaction, as described previously.

TC-PRISMA [8, 12] enables us to calculate the Time-Temperature-Precipitation TTP diagram of $M_{23}C_6$ carbide precipitation for this steel. The chemical composition of the austenite phase was calculated by Thermo-Calc using the Scheil module. This is very close to that of the real alloy composition. Additionally, the interfacial energy between γ and $M_{23}C_6$ was considered to be about 0.23 J/m^2, according to the literature [12].

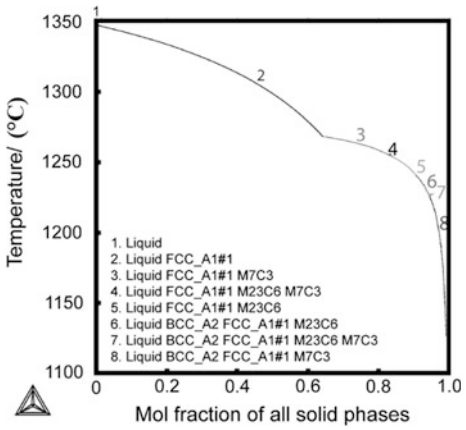

Fig. 6 Thermo-Calc calculated plot of temperature against mole fraction of the all solid phases calculated for the steel

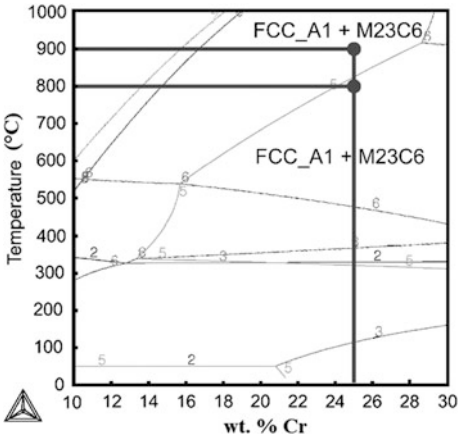

Fig. 7 Thermo-Calc calculated equilibrium pseudo binary Fe-Cr phase diagram of the steel

TC-PRISMA solves numerically the equation of the modified Langer-Schwartz theory [11] which consider that the nucleation, growth and coarsening of precipitates is concomitant. The solution can be completed using the N-model of Kapmann and Wagner [11]. The precipitation was considered to be a homogeneous nucleation process (bulk nucleation). TTP diagram is presented in Fig. 8 which indicates that the nucleation and growth kinetics of M23C6 precipitation in the austenite matrix occurs more rapidly at about 880 °C which is consistent with SEM microstructure of Fig. 1 which shows a faster kinetics of precipitation at about 900 °C than that of the other two temperatures, 700 and 800 °C.

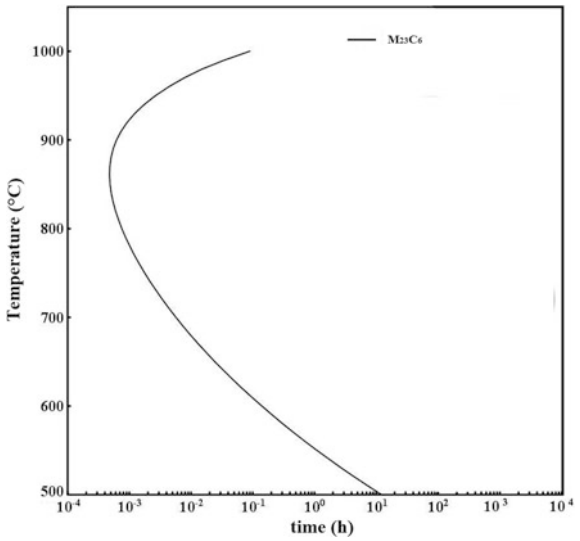

Fig. 8 TTP diagram of $M_{23}C_6$ precipitation for the steel

Conclusions

Thermo-Calc analysis of as-cast HK40 steel assessed correctly the non-equilibrium formed phases. These are mainly M_7C_3 carbides and austenite. Aging treatment at temperatures of 700, 800 and 900 °C for different times promoted the precipitation of $M_{23}C_6$ in the austenite matrix. PRISMA calculated TTP diagram for the $M_{23}C_6$ precipitation is consistent with the SEM observations of the aged steel.

Acknowledgements The authors wish to thank the financial support from SIP-COFAA-IPN and CONACYT.

References

1. Kaya AA (2002) Microstructure of HK40 alloy after high temperature service in oxidizing/carburizing environment, I. Oxidation phenomena and propagation of a crack. Mater Charact 49:11–21
2. Liu J, Jiao D, Luo C (2010) Microstructural evolution in austenitic heat-resistant cast steel 35Cr25Ni12NNbRe during long-term service. Mater Sci Eng A 527:2772–2779
3. Haro S, Lopez D, Velasco A (2000) Microstructural factors that determine the weldability of a high Cr-high Si HK40 alloy. Mater Chem Phys 66:90–96
4. Babakr AM, Al-Ahmrai A, Al-Jumayiah K (2009) Failure investigation of a furnace tube support. J Fail Anal Preven 9:16–22
5. ASTM Standard A351/A351 M–03 (2004) Standard specification for casting, austenitic, austenitic-ferritic (duplex), for pressure-containing parts. ASTM
6. Coreño-Alonso O, Duffus A, Sanchez C (2004) On the effect of σ-phase formation during metal dusting. Mater Chem Phys 84:20–28
7. Almeaida LH, Freitas A, Le May I (2003) Microstructural characterization of modified 25Cr-35Ni centrifugally cast steel furnace tubes. Mater Charact 49:219–229
8. Andersson JO, Helander T, Höglund L, Shi P, Sundman B (2002) Themo-Calc and Dictra. Comput Tools Mater Sci Calphad 26:273–312
9. Thermo-Calc software 2016b/tcfe7.tdb and mobFe2.ddb data
10. Kegg GR, Silcock JM (1972) The shape of M23C6 particles. Scr Metall 6:1083–1086
11. Kostorz G (2001) Phase tranformation in material. Wiley-VCH, Germany, pp 309–408
12. Pellizari M (2010) Thermodynamic modelling for the alloy design of high speed steels and high chromium cast irons. Mater Tech 44:121–127